Catalysis Science & Technology

PAPER

View Article Online
View Journal | View Issue

Cite this: *Catal. Sci. Technol.*, 2014, **4**, 1749

Cycloaddition of CO_2 and epoxides catalyzed by imidazolium bromides under mild conditions: influence of the cation on catalyst activity†

Michael H. Anthofer,‡[a] Michael E. Wilhelm,‡[a] Mirza Cokoja,*[a] Iulius I. E. Markovits,[a] Alexander Pöthig,[a] János Mink,[bc] Wolfgang A. Herrmann[a] and Fritz E. Kühn[a]

Received 7th December 2013,
Accepted 17th February 2014

DOI: 10.1039/c3cy01024d

www.rsc.org/catalysis

The synthesis and characterization of a library of imidazolium-based compounds of the type $[R^1R^2R^3im]Br$ (R^1 = H, CH_3, benzyl (Bz), 1-(2,3,4,5,6-pentafluoro)benzyl (Bz^{F5}); R^2 = H, CH_3, C_2H_5; R^3 = *n*-butyl, *n*-octyl) are reported. All compounds were characterized by means of ^1H and ^{13}C NMR spectroscopy, elemental analysis and single crystal X-ray diffraction in the case of 1-Bz^{F5}-3-*n*-octylimidazolium bromide and examined as catalysts for the cycloaddition of carbon dioxide and propylene oxide (PO) to yield propylene carbonate (PC). The catalyst screening shows the influence of different substituents (steric and ion pairing effects) on the catalytic activity. It is shown that the most active catalyst, 1-Bz^{F5}-3-*n*-octylimidazolium bromide (**10**), gives very good conversions and carbonate yields at 70 °C and below 5 bar CO_2 pressure, which is the lowest temperature for the synthesis of PC from PO and CO_2 using metal-free catalysts. Catalyst **10** can be recycled and reused at least 10 times without loss of yield and activity.

Introduction

Carbon dioxide may be considered as one of the key renewable carbon sources of the future, which could – provided sufficient energy or energy conserving processes are available – in the long term replace the currently exploited fossil carbon sources as a feedstock for the chemical industry.[1] Many concepts for the valorization of CO_2 are currently being discussed, among which CO_2 capture and recycling (CCR) is regarded to be the most promising one.[2–4] Nevertheless, CO_2 is an unreactive molecule, and its activation is associated with a considerable energy barrier. Further, CO_2 is one of the major greenhouse gases, which leads to the tempting misbelief that by CCR the CO_2 content in the atmosphere could (significantly) be reduced. Since the worldwide annual amount of anthropogenic CO_2 emission (industry, combustion, *etc.*) is more than a hundred times higher than the total amount of CO_2 used as reactant in the chemical industry, it is evident that CCR alone will most certainly not solve the 'greenhouse gas' problem in the foreseeable future. Hence, current research rather focuses on the question of how the CO_2 produced by human activities can be recycled and used as a C_1-feedstock without leaving a further carbon footprint. Several possibilities are being considered to reduce the industry- and technology-based CO_2 emission and to capture and store CO_2.[1,5] However, these concepts are either still in the nascent stage or they consume considerable amounts of energy, thus are far from large-scale applicability. For this reason, the development of high-performance molecular homogeneous catalysts is of particular interest, as they usually operate under much milder conditions compared to heterogeneous catalysts.[6,7]

To date, only few catalytic transformations of CO_2 in the homogeneous phase have the potential to be used on an industrial scale with positive CO_2 balance. One of them is the reaction of epoxides, above all the industrially important propylene oxide (PO),[8–10] with CO_2 to yield cyclic carbonates and polycarbonates. Particularly, propylene carbonate (PC) and poly(propylene carbonate) plastics are very important in industry.[8] As catalysts, mostly M–carboxylate, –salen and –porphyrin/–phthalocyanin complexes are used (M = Zn, Al, Sn, Cr, Fe, Co).[11–13] For the copolymerization of PO and CO_2, a wide variety of molecular transition metal catalysts is known.[14–18] Furthermore, the carbonate synthesis can be carried out without a metal catalyst as well, using nucleophilic reagents, such as halides or N-donor bases.[19] The use of halides is well documented, and meanwhile, ILs containing halides as anions or

---

[a] *Chair of Inorganic Chemistry/Molecular Catalysis, Catalysis Research Center, Technische Universität München, Ernst-Otto-Fischer-Straße 1, D-85747 Garching bei München, Germany. E-mail: mirza.cokoja@ch.tum.de; Fax: +49 89 289 13473; Tel: +49 89 289 13478*

[b] *Hungarian Academy of Sciences, Chemical Research Center, Pusztszeri u. 59-67, 1025 Budapest, Hungary*

[c] *Faculty of Information Technology, University of Pannonia, Egyetem u. 10, 8200 Veszprém, Hungary*

† Electronic supplementary information (ESI) available: X-ray single crystal data of compound **10**. CCDC 928238. For ESI and crystallographic data in CIF or other electronic format see DOI: 10.1039/c3cy01024d

‡ These authors have equally contributed to this work.

functionalized ILs are known to catalyze the cycloaddition, bearing the advantage of facilitated product separation due to the low volatility of the ILs.[19–23] Although metal-free catalysts are generally considered to be less active than molecular transition metal catalysts, they exhibit enormous potential regarding the introduction of functional groups and the tailoring of electronic properties, which even surpasses the portfolio of ligands for transition metal centers. Some examples of organocatalytic systems are covalent organic frameworks,[24] ionic liquids[19,25] and other supported catalytic matrices.[26–31] The most active organocatalysts, to date, are tandem catalysts containing phenol derivatives and nucleophiles (N-donor bases or halides), which are efficient even at temperatures below 45 °C.[32–35] The activity relies on the interaction of the hydroxyl group with the epoxide. In addition, new catalytic systems involving a cooperative or a carboxylic acid group and a nucleophilic reagent such as a halide or N-donor bases are known in the literature.[36] Yet, very often turnover frequencies (TOF) and numbers (TON) are not reported and catalyst recycling has not been studied. In the organocatalytic cycloaddition of CO_2 and epoxide, the efficiency of the reaction is mainly governed by the nucleophilicity of the catalyst.[37] In the first step of the reaction, a ring carbon atom of the epoxide is attacked by the nucleophile, yielding an alcoholate species. Subsequently, the alcoholate itself acts as a nucleophile, attacking the CO_2 carbon atom and resulting in the formation of an open carbonate intermediate, which undergoes 'back-biting', leading to the cyclic carbonate. Protic substituents at the catalyst, such as –COOH or –OH groups, can principally facilitate the ring opening by hydrogen bonding to the epoxide.[25,26,29]

Very recently, we have shown that in ionic liquid solutions, anions such as perrhenate $[ReO_4]^-$, which is notoriously unreactive in aqueous or organic solutions, show enhanced reactivity as nucleophiles, especially when the cation allows only weak ion pairing.[38] Our present study focuses on the effect of different substituents on imidazolium cations on the ion pairing, and the resulting effect on the nucleophilicity of the counterion and hence on the catalytic activity for the epoxide ring opening. Herein, we report the synthesis and characterization of a series of imidazolium bromides and their catalytic activity in the reaction of CO_2 and various epoxides to yield cyclic carbonates under mild conditions.

Experimental

General remarks

All preparations were carried out using standard techniques. Benzyl bromide, 2,3,4,5,6-pentafluorobenzyl bromide, 1-methylimidazole and 1-bromooctane were purchased from ABCR. Methyl iodide, imidazole, 1-butylimidazole, propylene oxide, styrene oxide, glycidol, cyclohexene oxide, epichlorohydrin and 1,2-epoxyoctane were purchased from Sigma Aldrich. All chemicals were used as received without further purification. All ionic liquids were dried under vacuum at 70 °C for 6 h.

Analytical equipment

Microanalyses of the obtained products were performed at the Mikroanalytisches Labor of the Technische Universität München in Garching using a HEKATech EURO EA. ^{1}H, ^{13}C, and ^{19}F NMR spectra were recorded in $CDCl_3$ or $[D_6]$-DMSO using a 400 MHz Bruker Avance DPX-400 spectrometer (400 MHz for ^{1}H, 101 MHz for ^{13}C, and 376 MHz for ^{19}F). IR spectra were recorded using a Varian IR FT670 that was equipped with an ATR cell (diamond crystal). Catalytic runs were monitored by gas chromatography using a Hewlett-Packard instrument HP 5890 Series II equipped with a FID, a Supelco column Alphadex 120 and a Hewlett-Packard integration unit 3396 Series II. The melting points of the compounds were determined using a melting point meter MPM-H2. The absorption of CO_2 in the ILs was determined by thermogravimetric analysis using a NETZSCH STA 409 PC. Fast Atom Bombardment (FAB) mass spectroscopy was carried out using a Finnigan MAT (type MAT90) with xenon as the ionization gas in a 3-nitrobenzyl alcohol matrix.

Synthesis of catalysts 1–10

1-Octylimidazole,[39] 1-methyl-2-ethylimidazole,[40] 1-methyl-3-butyl imidazolium bromide (**1**),[41] 1,2-dimethyl-3-butylimidazolium bromide (**2**),[42] 1-methyl-3-octylimidazolium bromide (**4**),[43] 1,2-dimethyl-3-octylimidazolium bromide (**5**),[44] 1-benzyl-3-butylimidazolium bromide (**7**),[45] and 1-(2,3,4,5,6-pentafluoro) benzyl-3-butylimidazolium bromide (**9**) (ref. 45) were synthesized according to literature procedures.

General synthesis of alkyl and benzyl substituted imidazolium bromides 3, 6 and 8

To a stirred solution of 10.0 mmol of imidazole in THF, 11.0 mmol of the alkyl bromide was added dropwise and the solution was refluxed for 24 h. The solvent was distilled and the resulting residue was washed with ether and ethyl acetate. After drying in vacuum at 70 °C for 6 h, the imidazolium bromides **3**, **6** and **8** were obtained.

1-Methyl-2-ethyl-3-butylimidazolium bromide (**3**): white solid; yield 90%; ^{1}H NMR (400 MHz, $CDCl_3$): δ(ppm) = 7.80 (d, ^3J(H,H) = 2.2 Hz, 1H, CH), 7.50 (d, ^3J(H,H) = 2.2 Hz, 1H, CH), 4.19 (t, ^3J(H,H) = 7.6 Hz, 2H, CH_2), 4.06 (s, 3H, NCH_3), 3.19 (q, ^3J(H,H) = 7.8 Hz, 2H, CH_2), 1.93–1.78 (m, 2H, CH_2), 1.50–1.36 (m, 2H, CH_2), 1.32 (t, ^3J(H,H) = 7.8 Hz, 3H, CH_3), 0.98 (t, ^3J(H,H) = 7.3 Hz, 3H, CH_3); ^{13}C NMR (101 MHz, $CDCl_3$): δ(ppm) = 123.72, 121.22, 48.75, 36.17, 32.45, 19.92, 17.93, 13.76, 11.86; m.p. 85 °C; elemental analysis (%): calcd. C 48.59, H 7.75, N 11.33, Br 32.3; found C 48.28, H 7.82, N 11.39, Br 31.1; MS (FAB): m/z calcd. for $[C_{10}H_{19}N_2^+]$ = 167.2; found 167.7.

1-Methyl-2-ethyl-3-octylimidazolium bromide (**6**): white solid; yield 86%; ^{1}H NMR (400 MHz, $CDCl_3$): δ(ppm) = 7.78 (d, ^3J(H,H) = 2.1 Hz, 1H, CH), 7.42 (d, ^3J(H,H) = 2.1 Hz, 1H, CH), 4.16 (t, ^3J(H,H) = 7.6 Hz, 2H, CH_2), 4.06 (s, 3H, CH_3), 3.19 (q, ^3J(H,H) = 7.7 Hz, 2H, CH_2), 1.86 (m, 2H, CH_2), 1.45–1.18 (m, 13H, CH_2, CH_3), 0.88 (t, ^3J(H,H) = 7.2 Hz, 3H, CH_3); ^{13}C NMR (101 MHz, $CDCl_3$): δ(ppm) = 123.74, 121.06, 49.01, 36.20, 31.86, 30.48, 29.22, 26.67, 22.78, 17.99, 14.28, 11.85; m.p. 54 °C; elemental analysis (%): calcd. C 55.44, H 8.97, N 9.24, Br 26.4; found C 55.40, H 9.13, N 9.12, Br 26.2; MS (FAB): *m*/*z* calcd. for $[C_{14}H_{27}N_2^+]$ = 223.2; found 223.8.

1-Benzyl-3-octylimidazolium bromide (**8**): white solid; yield 91%; ^{1}H NMR (400 MHz, $CDCl_3$): δ(ppm) = 11.01 (s, 1H, CH), 7.48–7.43 (m, 2H, arom.-H), 7.39 (m, 3H, arom.-H), 7.12 (s, 1H, CH), 7.10 (s, 1H, CH), 5.60 (s, 2H, CH_2), 4.28 (t, ^3J(H,H) = 7.5 Hz, 2H, CH_2), 1.90 (m, 2H, CH_2), 1.43–0.92 (m, 10H, CH_2), 0.85 (t, ^3J(H,H) = 6.7 Hz, 3H, CH_3); ^{13}C NMR (101 MHz, $CDCl_3$): δ(ppm) = 132.92, 129.86, 129.74, 129.29, 121.49, 53.75, 50.57, 31.84, 30.43, 29.21, 29.10, 26.48, 22.78, 14.28; m.p. 69 °C; elemental analysis (%): calcd. C 61.45, H 7.75, N 7.89, Br 22.7; found C 61.27, H 7.75, N 7.97, Br 22.9; MS (FAB): *m*/*z* calcd. for $[C_{18}H_{27}N_2^+]$ = 271.2; found 271.7.

Synthesis of 1-(2,3,4,5,6-pentafluoro)benzyl-3-octylimidazolium bromide (10)

To a stirred solution of 1.80 g of 1-octylimidazole (10.0 mmol, 1.0 equiv.) in THF, 2.87 g of 2,3,4,5,6-pentafluorobenzyl bromide (11.0 mmol, 1.1 equiv.) was added dropwise at 0 °C. After complete addition of the bromide, the solution was allowed to warm to r.t. and stirred for 24 h. The solvent was distilled off and the resulting residue was washed with ether and *n*-hexane. **10** was obtained as a white solid after drying in vacuum at 70 °C for 6 h (4.06 g, 9.2 mmol, 92%); since one signal of the backbone of the imidazolium ring was covered by the solvent signal, the spectra of **10** were recorded in DMSO-d6. ^{1}H NMR (400 MHz, $[D_6]$-DMSO): δ(ppm) = 9.30 (s, 1H, CH), 7.85 (s, 1H, CH), 7.81 (s, 1H, CH), 5.64 (s, 2H, CH_2), 4.16 (t, ^3J(H,H) = 7.2 Hz, 2H, CH_2), 1.77 (p, ^3J(H,H) = 7.1 Hz, 2H, CH_2), 1.33–1.11 (m, 10H, CH_2), 0.86 (t, ^3J(H,H) = 6.7 Hz, 3H, CH_3); ^{13}C NMR (101 MHz, $[D_6]$-DMSO): δ(ppm) = 136.63, 122.74, 49.03, 31.06, 29.18, 28.44, 28.21, 25.37, 22.01, 13.89; ^{19}F NMR (376 MHz, $[D_6]$-DMSO): δ(ppm) = −141.41 (dd, ^3J(F,F) = 22.9, 7.6 Hz), −152.84 (t, ^3J(F,F) = 22.9 Hz), −161.70 (td, ^3J(F,F) = 22.9, 7.6 Hz); m.p. 56 °C; elemental analysis (%): calcd. C 48.99, H 5.03, N 6.35, Br 18.1; found C 49.13, H 5.15, N 6.22, Br 18.7; MS (FAB): *m*/*z* calcd. for $[C_{18}H_{22}F_5N_2^+]$ = 361.2; found 361.6.

Experimental procedure for the catalytic conversion of CO_2 and epoxides

A Fisher–Porter bottle was charged with catalyst **10** (1.0 mmol) and equipped with a magnetic stirring bar. The epoxide (10.0 mmol) was added under Ar and the Fisher–Porter bottle was then placed under a constant pressure of CO_2 for 1 min and heated to the desired temperature. After reaction completion, the bottle was cooled down to 0 °C and the excess CO_2 was vented. The reaction mixture was collected by adding 5 mL of chloroform and a sample was collected for GC analysis to determine yield and selectivity.

For recycling studies, propylene carbonate was separated from the catalyst by adding a mixture of ethyl acetate and ether (1 : 4). The reaction mixture was dissolved in a minimum amount of ethyl acetate and afterwards the catalyst was precipitated by the addition of ether, whereas PC stayed in the organic layer and could be separated by evaporation of the solvent. The catalyst was dried at 70 °C for 6 h *in vacuo*. By adding the same amount of epoxide (10.0 mmol), the next catalytic run was started.

Determination of CO_2 solubility in ionic liquids 4, 5, 6, 8 and 10

An exact amount of IL was weighed in an aluminium oxide crucible and closed. The sample was heated *in vacuo* in the thermogravimetric analyzer for 30 min until a constant temperature was reached and the atmosphere was switched to CO_2 (1 bar). After 90 min, a constant mass was recorded and the weight increase was determined. Based on these values, the mole fraction CO_2 to IL was calculated as shown in Table 2.

Results and discussion

Synthesis and characterisation of imidazolium bromides 1–10

Imidazolium salts with varying alkyl group lengths, as well as with fluorinated substituents, were synthesized since it was reported that imidazolium-based ionic liquids with long alkyl chain moieties allow a higher solubility of CO_2.[46] Further, in order to avoid possible *in situ* formation of N-heterocyclic carbenes (NHC), the protons at the 2-position of the imidazolium ring were replaced by alkyl groups (Me, Et). All imidazolium bromide catalysts were prepared by treatment of a THF solution of an imidazole with the respective alkyl bromide (Scheme 1).

The purity of compounds **1–10** was determined by ^{1}H and ^{13}C NMR spectroscopy and elemental analysis (see the Experimental section). Further, the structure of compound **10** was confirmed by single crystal X-ray crystallography. The structure of **10** is shown in Fig. 1 and the intermolecular contacts in the solid state are depicted in Fig. 2. The crystal structure of **10** shows intermolecular hydrogen bonds between the imidazolium cation and bromide. Therefore, five different hydrogen–bromide interactions are observed. As expected, the strongest contact was obtained from the proton at C(1) of the imidazolium ring with a distance of 2.584 Å. This distance is comparable to the known crystal structure of **1**, where a value of 2.446 Å was observed.[47] Additionally, the backbone proton

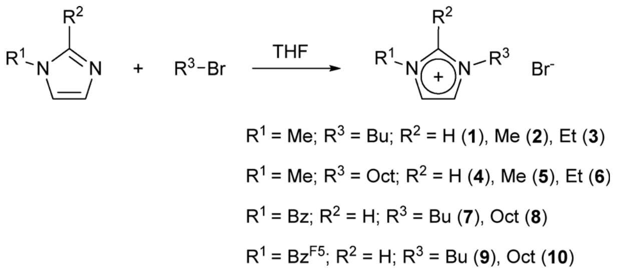

Scheme 1 General synthesis of the imidazolium bromide catalysts **1–10** (Me = methyl, Bu = *n*-butyl, Oct = *n*-octyl, Bz = benzyl, Bz^{F5} = 1-(2,3,4,5,6-pentafluoro)benzyl).

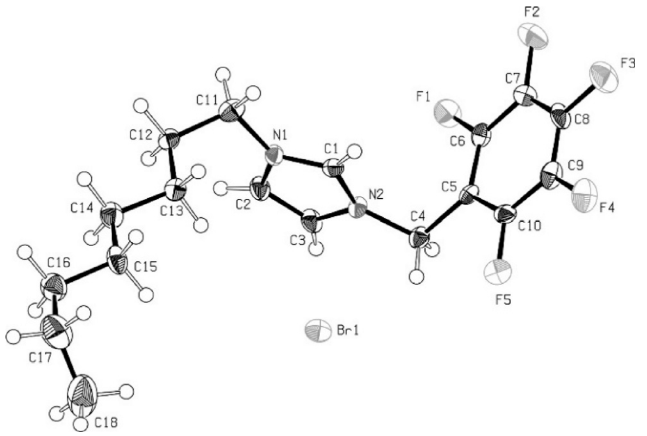

Fig. 1 ORTEP view of the structure of compound **10**. Thermal ellipsoids are shown at the level of 50% probability. Selected bond lengths (Å) and angles (°): C1–N1, 1.323(6); C1–N2, 1.325(6); C2–N1, 1.382(6); C3–N2, 1.375(6); C2–C3, 1.344(7); N1–C11, 1.468(6); N2–C4, 1.465(5); N1–C1–N2, 198.8(4); C1–N1–C2, 108.4(4); C1–N2–C3, 108.6(4); C3–C2–N1, 107.0(5); C2–C3–N2, 107.1(4); C1–N1–C11, 126.1(4); C1–N2–C4, 127.2(4); C1–N2–C4–C5, 36.0; C2–N1–C11–C12, 58.4.

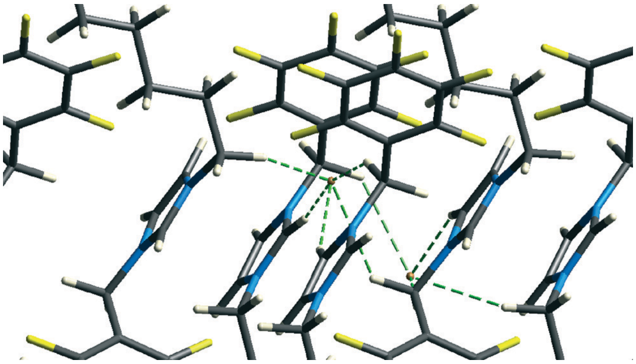

Fig. 2 Illustration of the crystal packing in compound **10** and the H⋯Br contacts.

at C(3) shows a rather strong interaction (2.685 Å). Weaker interactions were detected from a methylene proton at C(4) to Br$^-$ (distances, 2.800 Å and 2.939 Å) and even the *n*-octyl side chain shows interaction to the bromide from the proton at C(11) with a distance of 2.827 Å. These contacts were confirmed by Hirshfeld surface analysis (see the ESI,† Fig. F2).

Therefore, for a fluorinated bromide like **10**, the contact is quite strong compared to an imidazolium bromide bearing fluorinated and non-fluorinated aromatic side chains (distance, 2.750 Å).[48] In this case, no contact between the methylene protons of the BzF^5 moiety and Br$^-$ was observed. However, the methylene bridge of the Bz group shows hydrogen bonding to Br$^-$ with a distance of 2.884 Å and, hence, is in a similar range as determined for **10**. The backbone proton in the crystal structure of **1** shows a distance of 2.873 Å and therefore is longer than the observed distance in **10**. The first carbon atom of the *n*-butyl side chain showed a hydrogen bond to the bromide with a distance of 2.845 Å and is comparable to that in **10**.[47] Further, hydrogen bonding interactions between the fluorine atoms in *ortho*- and *para*-positions of the aromatic ring and the protons at C(3), C(13) and C(15) could be observed in the crystal structure.

Synthesis of PC from CO$_2$ and PO with catalysts 1–10

The screening of the catalytic activity of the synthesized imidazolium bromides **1–10** bearing aliphatic, benzyl or fluorinated benzyl wingtips (Scheme 1) was carried out using propylene oxide (PO) as the substrate for the cycloaddition of CO$_2$. Imidazolium-based ionic liquids are known to efficiently catalyse the cycloaddition of epoxides and CO$_2$.[22,23] The reactions were performed in neat PO without further solvents, since using solvents (chloroform, dimethyl carbonate, methyl ethyl ketone) has a detrimental effect on the catalytic activity. In a typical experiment, a Fisher–Porter bottle (pressure reaction glass vessel) was charged with the catalyst and PO (catalyst : substrate ratio 1 : 10) and then pressurized with 4 bar CO$_2$ for 1 min. Subsequently, the mixture was heated at 70 °C for 22 h. A reaction time of 22 h is necessary to reach 91% conversion of PO using **10** as the catalyst under the observed reaction conditions (Fig. 4). Based on these results, the catalyst screening was carried out for a reaction time of 22 h to compare catalysts **1–10** and therefore, get a better insight into the role of the cation on the catalytic activity. Note that at this temperature, all examined catalysts are liquid and PO is in the gas phase; hence, at the reaction temperature, the catalyst also acts as a solvent for the partially dissolved substrates. This allows the investigation of the influence of the substitution pattern of the cation of the different catalysts **1–10** without any solvent-related effects.

The conversion of PO was determined by gas chromatography (GC). The results of the screening are shown in Table 1. Overall, it can be seen that all organocatalysts are quite active, leading to good to very good conversions of PO with a high selectivity of PC. Due to the absence of water, the formation of 1,2-propanediol as a side product is suppressed, which is also observed in several other reports using ionic compounds as catalysts.[22,23] Note that the formation of polycarbonates has not been observed in any of our catalytic experiments.

The mechanism of the cycloaddition of epoxides with CO$_2$ using tetrabutylammonium halides as catalysts was shown in several reports.[37,49] The epoxide ring is opened by the halide, forming an oxyanion species, which reacts with CO$_2$ to yield a cyclic carbonate after intramolecular cyclic elimination (‘back-biting’). The mechanism with imidazolium halide catalysts follows an analogous reaction pathway and is illustrated in Scheme 2.[22,23]

In the absence of a catalyst, no PO conversion could be detected under the observed reaction conditions (70 °C, 4 bar CO$_2$ pressure, neat, 22 h). Regarding the PO conversions obtained with catalysts **1–3**, it is notable that substitution of the acidic ring proton at the 2-position by methyl and ethyl groups leads to a reduction of the conversion. The contact between the imidazolium ring proton at the C2-position and the epoxide oxygen atom facilitates the opening of the

Table 1 Synthesis of PC from CO_2 and PO using catalysts **1**–**10**

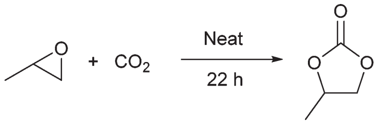

Cat.	mmol cat.	mmol PO	$p(CO_2)$ [bar]	T [°C]	Conv.[a] [%]	PC sel. [%]
—	0	10	4	70	0	—
1	1	10	4	70	85	>99
2	1	10	4	70	64	>99
3	1	10	4	70	69	>99
4	1	10	4	70	88	>99
5	1	10	4	70	80	>99
6	1	10	4	70	71	>99
7	1	10	4	70	77	>99
8	1	10	4	70	73	>99
9	1	10	4	70	86	>99
10	1	10	4	70	91	>99

[a] Conversion is based on GC analysis.

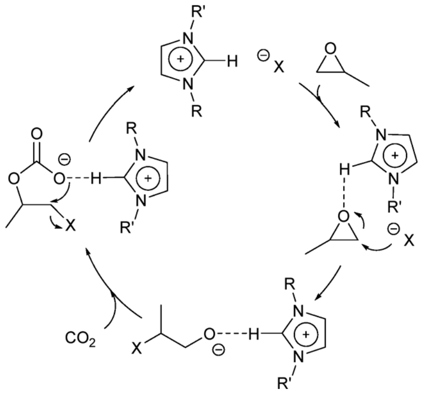

Scheme 2 Proposed mechanism for the cycloaddition of CO_2 with PO using an imidazolium halide catalyst.

epoxide ring by the nucleophilic bromide anion. When the proton is substituted by an alkyl group, this interaction does not exist anymore and hence, the relative catalytic activity is weaker. This trend is corroborated by the relative activities of the catalyst series **4**–**6**. In contrast, a non-fluorinated benzyl substituent does not exhibit any beneficial effect compared with the alkyl moieties (*cf.* catalysts **7**, **8** *vs.* **1**, **4**). A positive catalytic effect can be observed upon fluorinating the benzyl side chain. The best results were achieved with catalyst **10**, which bears one octyl group and one fluorinated benzyl group on the imidazolium ring N atoms (91%). These results are consistent with the fact that, in general, fluorinated cations increase the solubility of CO_2 in the ionic liquid phase.[50] Previous studies show that the CO_2 solubility in imidazolium-based ionic liquids largely depends on the nature of the anion, rather than that of the cation,[51] hinting that in our case the gas solubility does not have a significant impact on the different catalytic activities, since in all catalysts, the anion is bromide. Nevertheless, to shed some light on the actual impact of the CO_2 solubility in the reaction, the CO_2 solubility in the ILs **4**, **5**, **6**, **8** and **10** was determined at 70 °C and 1 bar CO_2 pressure using thermogravimetric analysis. The calculated mole fractions CO_2 to IL were calculated and listed in Table 2.

Table 2 CO_2 absorption of **4**, **5**, **6**, **8** and **10** at 70 °C under 1 bar CO_2 pressure using thermogravimetric analysis

Entry	IL	Mole fraction (χ) CO_2 to IL
1	**4**	0.058 ± 0.002
2	**5**	0.077 ± 0.003
3	**6**	0.109 ± 0.001
4	**8**	0.096 ± 0.004
5	**10**	0.102 ± 0.011

Very recently, Torralba-Calleja *et al.* presented a comprehensive summary of the solubility of CO_2 in various (imidazolium-based) ionic liquids.[52] Nonetheless, despite our best efforts, no data on imidazolium bromide ionic liquids could be found and therefore a direct comparison of the obtained results is difficult. For example, analogues of **1** and **4** with BF_4^- as the anion were examined under slightly different conditions (10 bar CO_2 pressure, 60 °C). These compounds show mole fractions (χ) of 0.0895 and 0.121 CO_2 to IL,[52] which corroborate the observation of better CO_2 solubility upon increasing the chain length and CO_2 pressure.[46] However, when more than one parameter is changed (temperature, pressure, anion), it is difficult to rank the obtained CO_2 solubilities in our catalyst in the series of existing data. The results show an increase of CO_2 solubility upon substitution at the C2-position of the imidazolium moiety in the order H (**4**) < Me (**5**) < Et (**6**), which does not point to a correlation between the CO_2 solubility and the catalytic activity. Furthermore, an aromatic wingtip (Table 2, entry 4) increases the solubility of CO_2 in the IL compared to a methyl group (Table 2, entry 1) and the fluorination of the aromatic ring (Table 2, entry 5) has only a small influence on the solubility of CO_2 in the IL. In summary, the investigated ILs only dissolve a small amount of CO_2 (approx. 1% compared to the used substrate) and their differences are not significant. Nevertheless, recent investigations indicate a significant impact of the cation structure on CO_2 capture in imidazolium-based ionic liquids.[53,54] Therefore, the impact on catalysis appears to be negligible, at least under the conditions applied in our experiments (70 °C, <5 bar CO_2). The presence of a proton at the C2-position of the imidazolium ring appears to have the largest impact on the PO conversion using catalysts **1**, **4** and **7**–**10**, followed by the steric demand of the substituents at C1- and C3-positions.

In order to exclude the formation of N-heterocyclic carbenes (NHC) during the reaction (resulting from deprotonation at the 2-position of the imidazolium ring), catalysts **2**, **3**, **5** and **6** bearing Me and Et groups were examined as well (see Scheme 1). It is well known that NHCs efficiently catalyse the cycloaddition of PO and CO_2.[55,56] If a free carbene was responsible for the catalysis, **2**, **3**, **5** and **6** would be (almost) inactive, which would result in poor conversion of PO. However, only a slight decrease of the PO conversion was observed and therefore, the formation of free NHCs during the reaction can be excluded. Nevertheless, apparently the acidic imidazolium proton has a high influence on the catalytic activity, which is manifested in the conversions (see Table 1). This effect is most presumably caused by hydrogen interactions between the imidazolium proton and the oxygen atoms of the epoxide, leading to a stronger polarization of the C–O bond and hence, to an increased electrophilicity of the epoxide carbon, facilitating the ring opening. Theoretical calculations support the assumption of strong interactions of the C2 proton of the imidazolium ring with the anion.[57,58] In addition, weaker interactions around the backbone protons with the anion are also found; however, they are less pronounced. Furthermore, substituting the C2 proton with a methyl group results in a different situation, where the anion is preferably located above and below the ring.[58] This is also observed using IR, Raman and NMR spectroscopy, showing changes in the electron density which are attributed to the position and strength of interionic interactions.[59] Additionally, interactions of the backbone with the anion are found and the probability of interactions of the carbon atom between the two nitrogen atoms with the anion is feasible. Interestingly, the simulations show no stronger ion pairing for unsubstituted ILs, whereas stronger hydrogen bonds can be formed compared to substituted ILs. According to the computational simulations, several possible interactions of PO with an imidazolium cation can be considered. By using neutron diffraction, it was shown that the interaction from the anion to the cation is dependent on the charge density and anion size.[60,61] Nonetheless, interactions between the hydrogen atoms at C2-, C4- and C5-positions and the anion are also detected in the liquid state. The access to the backbone protons can be restricted due to steric effects arising from long alkyl side chains.[62] Further examination of the role of a cation of an IL in nucleophilic S_N2 and S_NAr reactions show no clear effect of the degree of the cation substitution pattern on the reactivity.[63,64] No exact interaction site could be determined and the positive effect of ionic liquids on the outcome of the investigated reactions is generally considered to derive from their electrostatic influence.[63,64]

Nevertheless, based on the catalytic results, the cation has an influence on the cycloaddition of PO and CO_2, most probably due to different hydrogen bonding interactions of the IL with PO. Despite our best efforts, we have so far been unable to grow crystals of compound **10** from a PO solution to determine the existence of a H-contact of the C2-proton and PO in the solid state. In order to determine the hydrogen bonding character between **10** and PO, a FTIR study was carried out (Fig. 3). The IR spectrum of neat compound **10**, shown in Fig. 3a, exhibits a distinct vibration band at 3064 cm^{-1}, which becomes broader (from ~20 cm^{-1} to 60 cm^{-1} half width) and shifts to 3040 cm^{-1} upon addition of an excess of PO to **10** at room temperature. This frequency shift (24 cm^{-1}) can be ascribed to the intermolecular interaction of **10** and PO through hydrogen bonding. This band is assigned to the C–H stretching mode of the C2-position of the imidazolium ring (C(1) carbon in Fig. 1). It is reasonable to assume that this vibration is coupled with the stretching mode of the backbone C–H bonds (C(2) and C(3) carbons in Fig. 1) at 3134 cm^{-1}. Further, some out-of-plane deformation modes at 650 and 620 cm^{-1} also shift as a consequence of the interaction with PO. Several imidazolium-ring vibrations are shifted, which could all be responsible for the interaction with PO. This makes it difficult to exactly pinpoint which part or fragment of the cation interacts with PO. Nevertheless, the strongest interaction was observed between the acidic imidazolium proton and the oxygen atom of PO through hydrogen bonding (see Fig. 3).

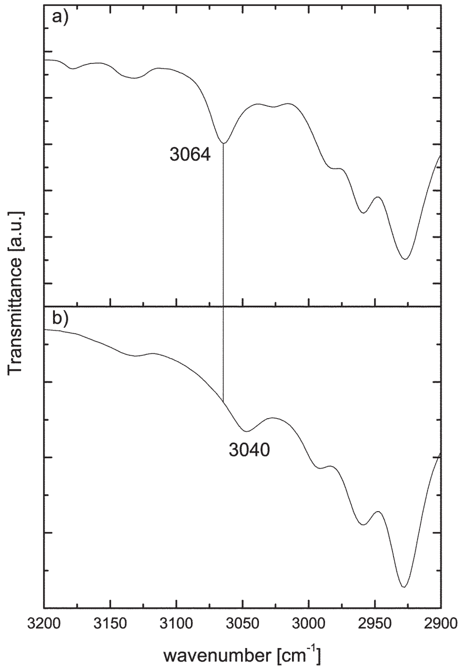

Fig. 3 FTIR spectra of a) neat compound **10** and b) **10** in the presence of excess PO between 3200 and 2900 cm^{-1}.

This interaction, leading to the weakening of the C–H bond, facilitates the nucleophilic attack of the bromide anion at the ring carbon and the epoxide ring opening. Consequently, increasing the acidity of the proton at the 2-position of the ring, *e.g.* by introducing electron-withdrawing substituents to the N ring atoms, would further strengthen this effect. It is noteworthy that with fluorination of the benzyl moiety (see catalysts **9** and **10**) the electron density in the imidazolium ring is reduced, leading to a stronger imidazolium–H···O–epoxide contact and hence, higher PO conversions. For this reason, further investigations, such as optimization of the reaction conditions, recycling studies and screening of different substrates, were carried out using the ionic liquid **10** (m.p. 56 °C) as the catalyst.

Kinetic studies

For a detailed insight into the reaction of PO and CO_2 using catalyst **10**, further investigations were carried out. In a row of nine identical experiments, each reaction was stopped after a defined time period and analysed by GC analysis and the conversion of PO was plotted *versus* the corresponding reaction time (Fig. 4). In comparison to the so far most efficient halide organocatalyst for this reaction, [HDBU]Cl (97% PC after 2 h at 140 °C, cat. conc. 1 mol%, 10 bar CO_2),[25] catalyst **10** is active at lower reaction temperature and CO_2 pressure, yet higher reaction time. To compare the efficiency of catalyst **10** with that of [HDBU]Cl (DBU = 1,8-diazabicyclo[5.4.0]undec-7-ene), the reaction was carried out under the same reaction conditions as described in ref. 25. A PO conversion of 91% with a selectivity of 99% towards PC was obtained, which is only slightly lower than that using [HDBU]Cl, thus rendering catalyst **10** comparable to the state-of-the-art. Lowering the pressure to 4 bar CO_2 reduces the conversion of PO to 64% after a 2 h reaction time.

In addition, the influence of temperature and catalyst loading on the carbonate yield was investigated. Upon lowering the temperature from 70 °C to 50 °C, the conversion of PO also decreased from 91% to 45% (Fig. 5).

Interestingly, the difference in the conversion of PO at a reaction temperature of 60 °C is only a little lower than at 70 °C, which may offer the opportunity to further reduce the temperature. A reduction of the catalyst concentration occurs along with a decrease of the catalytic activity, showing a nearly linear relationship between the catalyst concentration and the yield of propylene carbonate (Fig. 6). By lowering the catalyst loading to 1 mol%, the catalyst is still active, but the PO conversion decreases to 33%. Additionally, for a better understanding of the activity of the catalyst at different catalyst loadings the influence on the conversion of PO within the first 4 h of the reaction was monitored and compared. The dependence of the catalyst concentration on the activity (= turnover frequency, TOF) follows the order of 10 mol% > 5 mol% > 1 mol% (see Fig. 6 and 7).

Under the applied reaction conditions, 1 mol% catalyst results in very poor activity for the conversion of PO. The

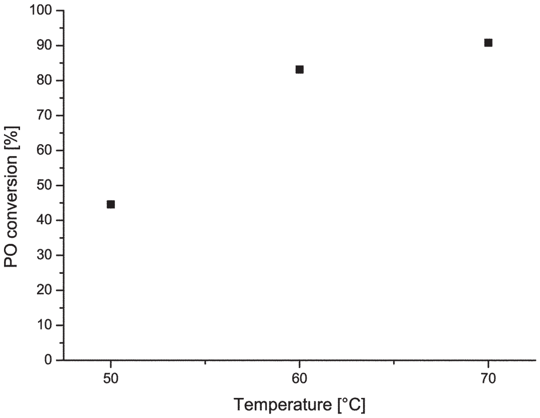

Fig. 5 Influence of the reaction temperature on the conversion of PO. Reaction conditions: 10 mmol of PO, 1 mmol of catalyst **10**, 4 bar CO_2, 22 h.

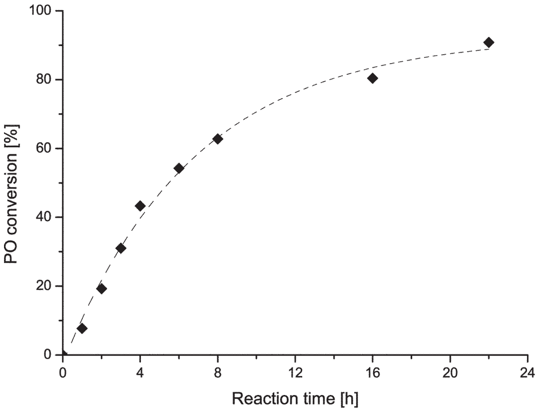

Fig. 4 Kinetic curve of the reaction of PO and CO_2 using catalyst **10**. Reaction conditions: 10 mmol of PO, 1 mmol of catalyst **10**, 4 bar CO_2, 70 °C.

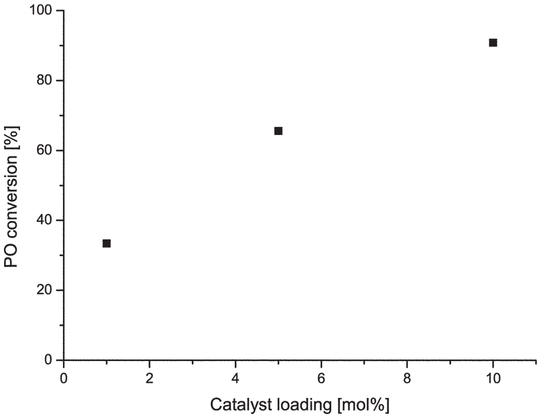

Fig. 6 Dependence of the concentration of catalyst **10** on the conversion of PO. Reaction conditions: 10 mmol of PO, 4 bar CO_2, 70 °C, 22 h.

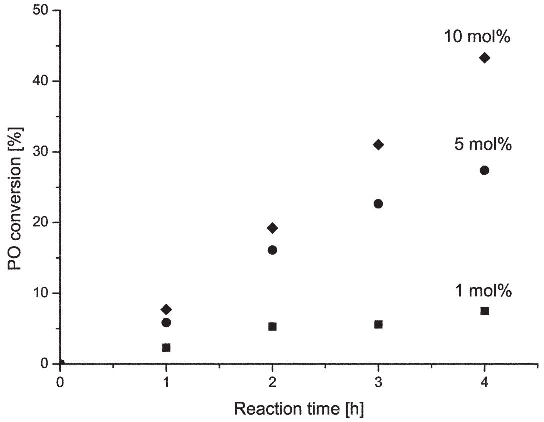

Fig. 7 Kinetic curve of the first 4 h with 10 mol%, 5 mol% and 1 mol% of catalyst **10**. Reaction conditions: 10 mmol of PO, 4 bar CO_2, 70 °C.

difference in the TOFs for catalyst loadings of 5 and 10 mol% is somewhat smaller; however, the trend is already clear at an early stage of the reaction (1 h). Notably, a higher reaction temperature and CO_2 pressure have a more pronounced impact on the activity. As stated below, at 140 °C, 10 bar CO_2 and only 1 mol% catalyst **10**, after 2 h, a conversion of 91% is reached (*vide supra*), showing that the decisive parameter is not the catalyst concentration (*cf.* 5% conversion with 10 mol% 10 at 70 °C and 4 bar CO_2). On the other hand, it can be argued that the more favourable scenario would be shorter reaction times but harsher reaction conditions (taking into account the carbon footprint) or milder conditions associated with longer reaction times.

Recycling studies

Stability and recyclability of a catalyst are of great importance for an application beyond the laboratory scale. In order to examine the reusability of catalyst **10** after separation of the product and to exclude possible leaching effects, the catalytic cycloaddition of PO and CO_2 was carried out under the conditions described above. After separation of PC from the catalyst by extraction with ethyl acetate/diethyl ether (for details see the Experimental section) the catalyst was dried and used for the next run under the same conditions. The results, shown in Fig. 8, indicate that the conversion of PO remains stable after ten consecutive cycles. The slight differences in the conversion lie in the range of the standard deviation of the gas chromatograph. From this, it can be stated that catalyst **10** may indeed be a suitable candidate for long-term catalysis experiments. Furthermore, leaching of the catalyst was not observed.

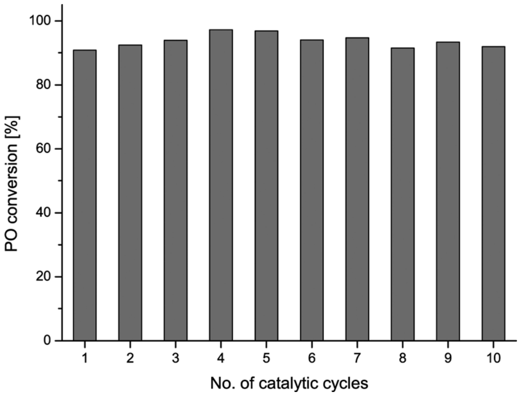

Fig. 8 Studies of the influence of catalyst recycling on the activity and PC yield. Reaction conditions: 10 mmol of PO, 1 mmol of catalyst **10**, 4 bar CO_2, 70 °C, 22 h. Conversions are based on GC analysis. PC selectivity: ≥99%.

Table 3 Catalyzed cycloaddition of different epoxides using catalyst **10** under optimized reaction conditions[a]

Entry	Substrate	Conv. [%]
1	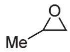	91[b]
2	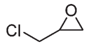	99[c]
3	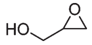	98[c]
4	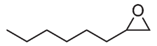	72[c]
5	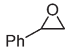	96[c]
6	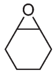	78[c]

[a] 10 mmol of epoxide, 1 mmol of catalyst **10**, 4 bar CO_2, 70 °C, 22 h. [b] Conversion is based on GC analysis; selectivity ≥99% for the carbonate product. [c] Conversions are based on ^1H NMR using mesitylene as the internal standard. Carbonate selectivity: ≥99%.

Conversion of CO_2 with other substrates

In order to show the potential of the new imidazolium catalyst **10**, the scope of epoxide substrates for the cycloaddition with CO_2 is extended (Table 3). Compound **10** is an efficient catalyst for the conversion of a variety of substrates with either electron withdrawing, electron donating or sterically encumbering substituents. For each experiment, the carbonate selectivity is ≥99%. The good conversions of epichlorohydrin and glycidol (entries 2 and 3; 99 and 98%, respectively) can be explained by their good electron-withdrawing capability, allowing for an easier nucleophilic attack of the epoxide ring carbon atoms. Even for cyclohexene oxide (entry 6), which is known to be notoriously more difficult to undergo cycloaddition than epoxides of open-chained terminal olefins, the corresponding carbonate is obtained in good yield.[22]

Conclusion

The new imidazolium-based ionic liquid **10** catalyses the transformation of CO_2 to cyclic carbonates under mild conditions. It is the first imidazolium-based organocatalyst which shows nearly quantitative conversion of propylene oxide to propylene carbonate below 80 °C and 5 bar CO_2. The absence of metals and additional solvents as well as the facile recycling and reusability without loss of activity render this catalyst particularly 'green'. The catalytic system can be reused at least ten times without any loss of catalytic activity. These results render compound **10** as a viable catalyst for CO_2 fixation with respect to a low carbon footprint. With the right choice of the substitution pattern at the imidazolium ring, the solubility towards CO_2 is enhanced. The effect of 'wingtip' substituents at the imidazolium ring on the acidity (and hence on the epoxide ring activation) on one hand and the ion pairing effect on the halide nucleophilicity on the other hand has been investigated. Further research efforts should focus on experimental and theoretical studies of the interplay between the hydrogen bonding, the acidity of the imidazolium salts, and the electronic and steric effects of the substituents, as well as on studies of the influence of CO_2 solubility on the catalytic activity. These studies aim at the development of ionic liquids with tailor-made cations, which should further facilitate the cycloaddition, allowing for a decrease of the reaction temperature below 70 °C (down to room temperature) and thus helping to minimize the carbon footprint for this reaction.

Acknowledgements

MHA, MEW and IIEM thank the TUM Graduate School for financial support.

Notes and references

1 M. Peters, B. Köhler, W. Kuckshinrichs, W. Leitner, P. Markewitz and T. E. Müller, *ChemSusChem*, 2011, **4**, 1216–1240.

2 N. MacDowell, N. Florin, A. Buchard, J. Hallett, A. Galindo, G. Jackson, C. S. Adjiman, C. K. Williams, N. Shah and P. Fennell, *Energy Environ. Sci.*, 2010, **3**, 1645–1669.

3 M. Mikkelsen, M. Jorgensen and F. C. Krebs, *Energy Environ. Sci.*, 2010, **3**, 43–81.

4 P. Markewitz, W. Kuckshinrichs, W. Leitner, J. Linssen, P. Zapp, R. Bongartz, A. Schreiber and T. E. Muller, *Energy Environ. Sci.*, 2012, **5**, 7281–7305.

5 E. A. Quadrelli, G. Centi, J.-L. Duplan and S. Perathoner, *ChemSusChem*, 2011, **4**, 1194–1215.

6 M. Cokoja, C. Bruckmeier, B. Rieger, W. A. Herrmann and F. E. Kühn, *Angew. Chem., Int. Ed.*, 2011, **50**, 8510–8537.

7 M. Drees, M. Cokoja and F. E. Kühn, *ChemCatChem*, 2012, **4**, 1703–1712.

8 T. Sakakura and K. Kohno, *Chem. Commun.*, 2009, 1312–1330.

9 W.-L. Dai, S.-L. Luo, S.-F. Yin and C.-T. Au, *Appl. Catal., A*, 2009, **366**, 2–12.

10 S. Fukuoka, M. Kawamura, K. Komiya, M. Tojo, H. Hachiya, K. Hasegawa, M. Aminaka, H. Okamoto, I. Fukawa and S. Konno, *Green Chem.*, 2003, **5**, 497–507.

11 A. Decortes, A. M. Castilla and A. W. Kleij, *Angew. Chem., Int. Ed.*, 2010, **49**, 9822–9837.

12 S. Klaus, M. W. Lehenmeier, C. E. Anderson and B. Rieger, *Coord. Chem. Rev.*, 2011, **255**, 1460–1479.

13 M. North, R. Pasquale and C. Young, *Green Chem.*, 2010, **12**, 1514–1539.

14 D. J. Darensbourg, *Chem. Rev.*, 2007, **107**, 2388–2410.

15 M. R. Kember, A. Buchard and C. K. Williams, *Chem. Commun.*, 2011, **47**, 141–163.

16 X.-B. Lu and D. J. Darensbourg, *Chem. Soc. Rev.*, 2012, **41**, 1462–1484.

17 X.-B. Lu, W.-M. Ren and G.-P. Wu, *Acc. Chem. Res.*, 2012, **45**, 1721–1735.

18 C. Chatterjee and M. H. Chisholm, *Chem. Rec.*, 2013, **13**, 549–560.

19 Z.-Z. Yang, Y.-N. Zhao and L.-N. He, *RSC Adv.*, 2011, **1**, 545–567.

20 Y. J. Kim and R. S. Varma, *J. Org. Chem.*, 2005, **70**, 7882–7891.

21 J. Sun, S.-I. Fujita and M. Arai, *J. Organomet. Chem.*, 2005, **690**, 3490–3497.

22 M. H. Anthofer, M. E. Wilhelm, M. Cokoja and F. E. Kühn, in *Transformation and Utilization of Carbon Dioxide*, ed. B. M. Bhanage and M. Arai, Springer, in print.

23 Q. He, J. O'Brien, K. Kitselman, L. Tompkins, G. Curtis and F. M. Kerton, *Catal. Sci. Technol.*, 2014, DOI: 10.1039/C3CY00998J.

24 J. Roeser, K. Kailasam and A. Thomas, *ChemSusChem*, 2012, **5**, 1793–1799.

25 Z.-Z. Yang, L.-N. He, C.-X. Miao and S. Chanfreau, *Adv. Synth. Catal.*, 2010, **352**, 2233–2240.

26 Y. Xiong, H. Wang, R. Wang, Y. Yan, B. Zheng and Y. Wang, *Chem. Commun.*, 2010, **46**, 3399–3401.

27 L. Han, H.-J. Choi, D.-K. Kim, S.-W. Park, B. Liu and D.-W. Park, *J. Mol. Catal. A: Chem.*, 2011, **338**, 58–64.

28 L. Han, H. Li, S.-J. Choi, M.-S. Park, S.-M. Lee, Y.-J. Kim and D.-W. Park, *Appl. Catal., A*, 2012, **429–430**, 67–72.

29 K. Motokura, S. Itagaki, Y. Iwasawa, A. Miyaji and T. Baba, *Green Chem.*, 2009, **11**, 1876–1880.

30 T. Sakai, Y. Tsutsumi and T. Ema, *Green Chem.*, 2008, **10**, 337–341.

31 Y. Xie, Z. Zhang, T. Jiang, J. He, B. Han, T. Wu and K. Ding, *Angew. Chem., Int. Ed.*, 2007, **46**, 7255–7258.

32 J. Sun, S. Zhang, W. Cheng and J. Ren, *Tetrahedron Lett.*, 2008, **49**, 3588–3591.

33 Y.-M. Shen, W.-L. Duan and M. Shi, *Eur. J. Org. Chem.*, 2004, **2004**, 3080–3089.

34 Y.-M. Shen, W.-L. Duan and M. Shi, *Adv. Synth. Catal.*, 2003, **345**, 337–340.

35 C. J. Whiteoak, A. Nova, F. Maseras and A. W. Kleij, *ChemSusChem*, 2012, **5**, 2032–2038.

36 J. Sun, L. Han, W. Cheng, J. Wang, X. Zhang and S. Zhang, *ChemSusChem*, 2011, **4**, 502–507.

37 J.-Q. Wang, K. Dong, W.-G. Cheng, J. Sun and S.-J. Zhang, *Catal. Sci. Technol.*, 2012, **2**, 1480–1484.

38 I. I. E. Markovits, W. A. Eger, S. Yue, M. Cokoja, C. J. Münchmeyer, B. Zhang, M.-D. Zhou, A. Genest, J. Mink, S.-L. Zang, N. Rösch and F. E. Kühn, *Chem. – Eur. J.*, 2013, **19**, 5972–5979.

39 M. Lee, U. H. Choi, S. Wi, C. Slebodnick, R. H. Colby and H. W. Gibson, *J. Mater. Chem.*, 2011, **21**, 12280–12287.

40 M. Debdab, F. Mongin and J. P. Bazureau, *Synthesis*, 2006, 4046–4052.

41 P. Lucas, N. E. Mehdi, H. A. Ho, D. Bélanger and L. Breau, *Synthesis*, 2000, 1253–1258.

42 C. C. Weber, A. F. Masters and T. Maschmeyer, *J. Phys. Chem. B*, 2012, **116**, 1858–1864.

43 I. Arellano, J. Guarino, F. Paredes and S. Arco, *J. Therm. Anal. Calorim.*, 2011, **103**, 725–730.

44 C. Betti, D. Landini and A. Maia, *Tetrahedron*, 2008, **64**, 1689–1695.

45 F. D'Anna, S. Marullo, P. Vitale and R. Noto, *ChemPhysChem*, 2012, **13**, 1877–1884.

46 S. N. V. K. Aki, B. R. Mellein, E. M. Saurer and J. F. Brennecke, *J. Phys. Chem. B*, 2004, **108**, 20355–20365.

47 J. D. Holbrey, W. M. Reichert, M. Nieuwenhuyzen, S. Johnson, K. R. Seddon and R. D. Rogers, *Chem. Commun.*, 2003, 1636–1637.

48 J. M. Serrano-Becerra, S. Hernandez-Ortega, D. Morales-Morales and J. Valdes-Martinez, *CrystEngComm*, 2009, **11**, 226–228.

49 V. Caló, A. Nacci, A. Monopoli and A. Fanizzi, *Org. Lett.*, 2002, **4**, 2561–2563.

50 M. J. Muldoon, S. N. V. K. Aki, J. L. Anderson, J. K. Dixon and J. F. Brennecke, *J. Phys. Chem. B*, 2007, **111**, 9001–9009.

51 C. Cadena, J. L. Anthony, J. K. Shah, T. I. Morrow, J. F. Brennecke and E. J. Maginn, *J. Am. Chem. Soc.*, 2004, **126**, 5300–5308.

52 E. Torralba-Calleja, J. Skinner and D. Gutirrez-Tauste, *J. Chem.*, 2013, **2013**, 1–16.

53 M. C. Corvo, J. Sardinha, S. C. Menezes, S. Einloft, M. Seferin, J. Dupont, T. Casimiro and E. J. Cabrita, *Angew. Chem., Int. Ed.*, 2013, **52**, 13024–13027.

54 O. Hollóczki, Z. Kelemen, L. Könczöl, D. Szieberth, L. Nyulászi, A. Stark and B. Kirchner, *ChemPhysChem*, 2013, **14**, 315–320.

55 H. Zhou, W.-Z. Zhang, C.-H. Liu, J.-P. Qu and X.-B. Lu, *J. Org. Chem.*, 2008, **73**, 8039–8044.

56 Y. Kayaki, M. Yamamoto and T. Ikariya, *Angew. Chem., Int. Ed.*, 2009, **48**, 4194–4197.

57 K. Fumino, A. Wulf and R. Ludwig, *Angew. Chem., Int. Ed.*, 2008, **47**, 8731–8734.

58 Y. Zhang and E. J. Maginn, *Phys. Chem. Chem. Phys.*, 2012, **14**, 12157–12164.

59 K. Noack, P. S. Schulz, N. Paape, J. Kiefer, P. Wasserscheid and A. Leipertz, *Phys. Chem. Chem. Phys.*, 2010, **12**, 14153–14161.

60 C. Hardacre, J. D. Holbrey, S. E. J. McMath, D. T. Bowron and A. K. Soper, *J. Chem. Phys.*, 2003, **118**, 273–278.

61 M. Deetlefs, C. Hardacre, M. Nieuwenhuyzen, A. A. H. Padua, O. Sheppard and A. K. Soper, *J. Phys. Chem. B*, 2006, **110**, 12055–12061.

62 C. Hardacre, J. D. Holbrey, C. L. Mullan, T. G. A. Youngs and D. T. Bowron, *J. Chem. Phys.*, 2010, **133**, 074510.

63 E. E. L. Tanner, H. M. Yau, R. R. Hawker, A. K. Croft and J. B. Harper, *Org. Biomol. Chem.*, 2013, **11**, 6170–6175.

64 E. E. L. Tanner, R. R. Hawker, H. M. Yau, A. K. Croft and J. B. Harper, *Org. Biomol. Chem.*, 2013, **11**, 7516–7521.